Proceedings of the International Symposium on Engineering Lessons Learned from
the 2011 Great East Japan Earthquake, March 1-4, 2012, Tokyo, Japan

EFFECTIVE STRESS ANALYSES OF TWO SITES WITH DIFFERENT EXTENT OF LIQUEFACTION DURING EAST JAPAN EARTHQUAKE

Hideki FUNAHARA[1], Sadayuki ISHIZAKI[2] and Toshiaki NAGAO[3]

[1] Senior Research Engineer, Technology Center, Taisei Corporation, Yokohama, Japan,
hideki.funahara@sakura.taisei.co.jp
[2] Research Engineer, Technology Center, Taisei Corporation, Yokohama, Japan,
sada.ishizaki@sakura.taisei.co.jp
[3] Chief Research Engineer, Technology Center, Taisei Corporation, Yokohama, Japan,
toshiaki.nagao@sakura.taisei.co.jp

ABSTRACT: The liquefaction extent observed along the Tokyo bay coast during the Great East Japan earthquake drastically differed depending on its location. Two locations in reclaimed areas, which have similar soil profiles, showed different liquefaction extent (i.e. One location heavily liquefied and another did not.). In this study, we employed a dynamic effective stress analysis technique to simulate the difference of the seismic behaviors of the two sites. The simulation implies a possibility that the liquefaction resistance at large cyclic numbers could affect the liquefaction occurrence due to the relatively small but long input motion.

Key Words: Great East Japan earthquake, liquefaction, effective stress analysis, reclaimed area of Tokyo bay coast, long duration of seismic motion

INTRODUCTION

The soil liquefaction was widely observed during the Great East Japan earthquake. Especially the liquefaction along the Tokyo bay coast received a lot of attention because the distances from the epicenter were long and the seismic intensities around the liquefied locations were relatively small. It is pointed out that the long duration of the seismic motion due to the large magnitude of the earthquake could be an important factor of the heavy liquefaction occurrence.

On the other hand, the liquefaction extent differed depending on the locations in reclaimed areas. The factors that affected the liquefaction extent could be the grain size distributions of the soil, the reclamation histories, the soil structure below the reclaimed layers and/or soil improvement works. However, the whole picture is not still understood precisely.

In this study, we look at two locations that showed different behaviors from the viewpoint of liquefaction occurrence. In order to estimate the seismic behaviors of the ground like pore water pressures, we conducted dynamic analyses using an effective stress analysis program. The focused factors are the modeling of the liquefaction strength curve and the small but long input motion.

OUTLINE OF THE TWO LOCATIONS

The first location (Site A) is Shin-Kiba, Koto ward and the second location (Site B) is Rinkai-cho, Edogawa ward. As shown in Figure 1, the two sites are in reclaimed areas around the Arakawa river mouth and located on opposite sides. The distance between the two sites is about 2 km.

The ground at site A heavily liquefied and many sand boils were observed (Photo 1). Many small buildings such as one or two-story offices, which probably sit on shallow foundations, suffered differential settlements. On the other hand, no liquefaction and no structural damage were observed around site B.

Fig. 1 Locations of the two sites studied in this research (Google maps)

Photo 1 Sand boils observed in Shin-Kiba area

Figure 2 shows the geological logs, the SPT-N values and PS logs of site A and B. The soil profiles consist of the upper landfill layer, loose alluvial sandy layer (upper Yurakucho layer, 10-14 m thickness), soft alluvial clayey layer (lower Yurakucho layer, about 20 m thickness), and relatively dense alluvial sandy layer (Nanagochi layer, 8 m thickness at site A, 20 m thickness at site B). The firm diluvial layer that has SPT-N value of more than 50 appears at the depth of 44 m (site A) and at the depth of 56 m (site B).

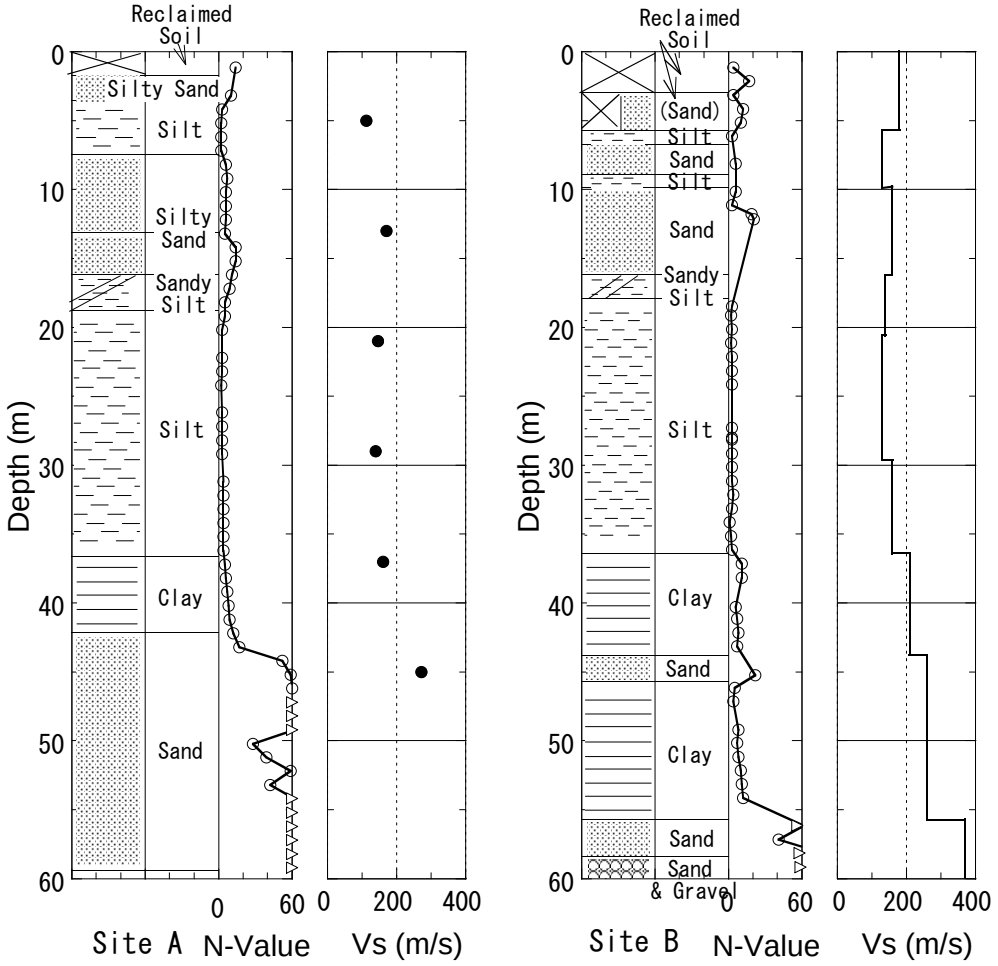

Fig. 2 Geological columns and PS logs

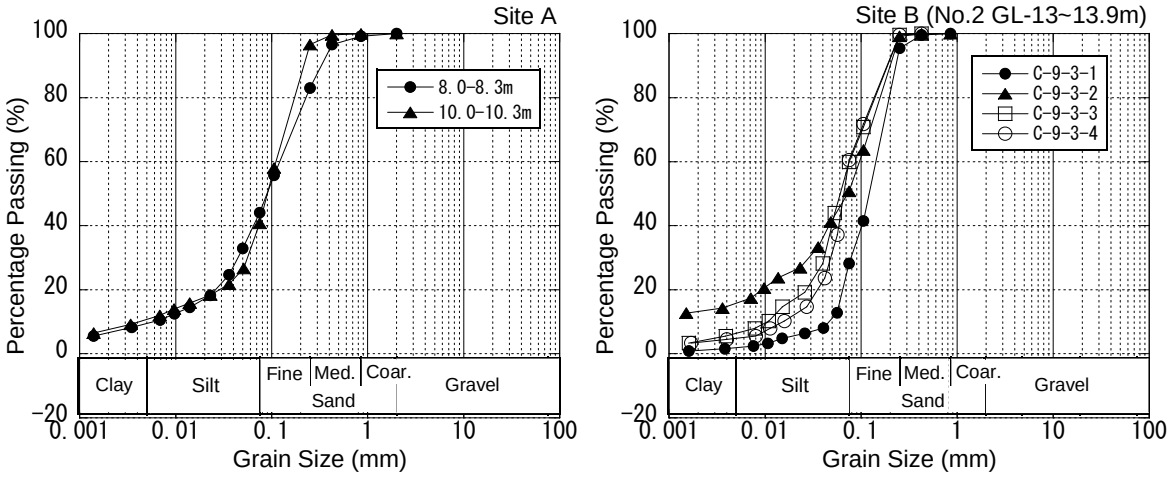

Fig. 3 Grain size accumulation curve

The boring logs for the two sites imply the liquefaction susceptibility of the reclaimed surface layer and the loose alluvial sandy layer. Figure 3 and Table 1 present the grain size

distribution curves and several characteristics of those liquefiable layers. The characteristics of the grain size distributions are mostly similar between the two sites, except the difference of the uniformity coefficient.

The fines contents of most samples exceed 35%, which is the upper limit of the liquefaction susceptible candidate for natural deposits in AIJ recommendations (Architectural Institute of Japan 2001).

According to several geotechnical surveyors, it is difficult to draw a borderline between a man-made layer reclaimed by dredging and the underlying natural deposit. Therefore, there is a possibility that some soil layers that is expressed like natural deposits in Figure 2 might be reclaimed layers. If this possibility is true, the silt layers could be liquefiable. However, at this stage, there is not any reliable evidence to change the natural silt to a liquefiable reclaimed soil. Therefore, in this study, we would assume that the soil less than 50% fines or less than 10% clays could be liquefiable.

Table 1 Characteristics of grain size distributions

	Site A		Site B (No.2 GL-13～14m)			
	8m	10m	1	2	3	4
D_{50}(mm)	0.0904	0.0911	0.1221	0.0731	0.0598	0.0659
Fc(%)	44	41	28.2	50.7	59.9	60.5
Pc(%)	9	11	1.9	15.3	6.2	4.5
Uc	19.31	26.31	2.78	--	7.04	4.84

D_{50}: Average Grain Size, *Fc*: fine fraction content
Pc: Clay fraction content , *Uc*: uniformity Coefficient

SIMPLIFIED LIQUEFACTION ASSESSMENT

Based on a method recommended in AIJ recommendations (Architectural Institute of Japan 2001), simplified liquefaction assessments were conducted. This method utilizes SPT-N value and fines content to estimate the liquefaction resistance of the ground. The Magnitude of 9.0 and the ground peak acceleration of 150 cm/s^2 are assumed considering the earthquake records obtained through K-net (http://www.kyoshin.bosai.go.jp/kyoshin/). The layers that contain more than 50% fines and more than 10% clay are considered as non-liquefiable layers.

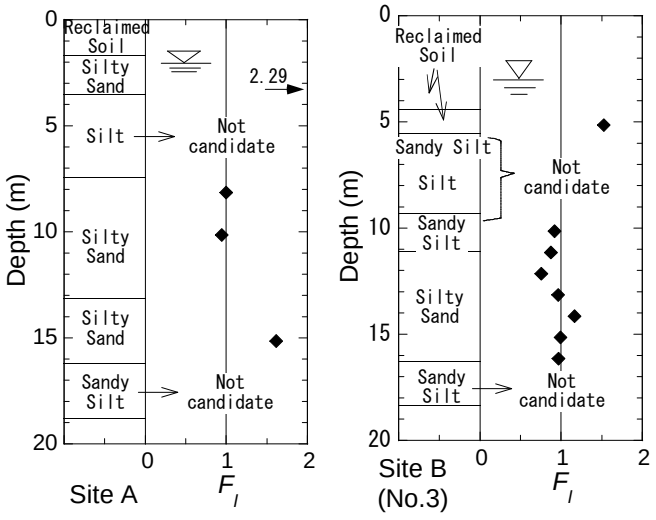

Fig.4 Computed safety factors against liquefaction

Figure 4 shows the results of liquefaction assessment. The computed safety factors against liquefaction (F_l) are less than 1.0 at several depths for both sites. In other words, the assessments predict the occurrence of liquefaction for both sites. However, in reality, the liquefaction was not observed at site B.

The cyclic displacement of ground surface (Dcy) can be estimated based on the simplified liquefaction assessment, and Dcy implies the extent of liquefaction. The estimated Dcy for site A is 2.5 cm that means the liquefaction extent is slight. On the other hand, the estimated Dcy for site B is 7.0 cm that means the liquefaction extent is small. The assessment for site A predicts the liquefaction occurrence itself. However, considering the amount of sand boils observed at the site, Dcy for site A could be underestimation.

DYNAMIC EFFECTIVE STRESS ANALYSES

Purpose of the dynamic analyses

The seismic motion during the Great East Japan earthquake continued for long duration. However, the simplified assessment mentioned above would have limits to be applied to such a long seismic motion. Therefore, in order to evaluate the dynamic behavior of soil, such as pore water pressure accumulation, acceleration, deformation etc., we conducted dynamic analyses utilizing an effective stress analysis program.

Numerical modeling

Outline of the modeling

The employed computation program is 'TDAPIII'. The numerical model is one dimensional soil column that consists of plane strain elements.

Modeling of non-liquefiable soil

The constitutive model for non-liquefiable layers is 'Modified Ramberg-Osgood Model'. Figure 5 presents the employed curves of shear strain dependency of shear stiffness and damping ratio. For site A, typical relations published in a reference (Architectural Institute of Japan 2006) are used. On the other hand, for site B, the laboratory testing data was available and targeted for modeling.

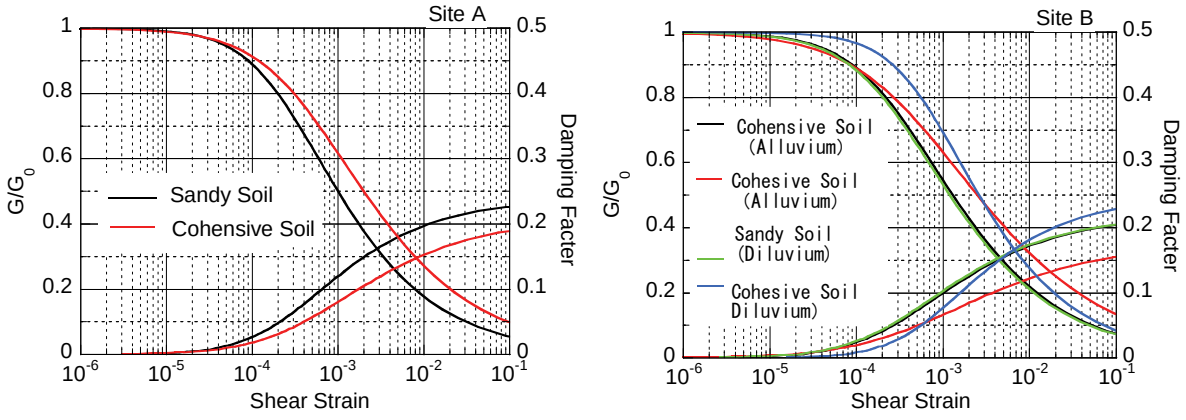

Fig. 5 Models of dynamic deformation characteristics

Modeling of liquefiable soil

The constitutive model for liquefiable layers is 'Stress-Density model' (Cubrinovski 1998a, Cubrinovski 1998b). The important target for modeling of the constitutive model is a liquefaction

strength curve. Figure 6 presents the liquefaction strength curves of the model. We had liquefaction testing data only for site B. Therefore, the testing data of site B was used as targets for modeling. On the other hand, for site A, we employed the parameters determined for Toyoura sand and adjusted the void ratio to fit the liquefaction strength at cyclic number of 15 that is computed in the simplified assessment mentioned above.

The essential difference of the liquefaction strength curves of the models at site A and site B should be looked at here, because the difference would affect the computed liquefaction behaviors afterward. The liquefaction strength curve of site A is slightly lower than the curve of site B as a result. Especially the difference is large at the large cyclic numbers. The modeling of the soil at site A is conducted simply by fitting the liquefaction strength at the cyclic number of 15 and the other cyclic numbers are not cared. On the other hand, when modeling the soil at site B, the whole averaged shape of the scattered liquefaction strength data are targeted and the inclination of the liquefaction strength curve is controlled.

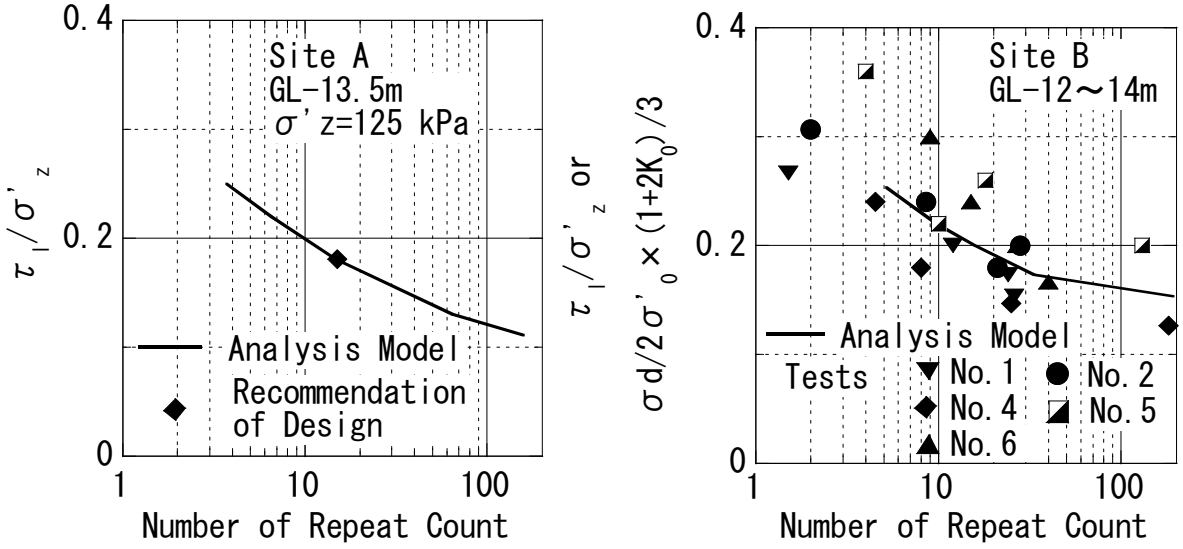

Fig.6 Models of liquefaction resistance curves

Input motion

As the input acceleration at the engineering bedrock for the dynamic analyses, a seismic record obtained by Port and Airport Research Institute (PARI) at Ooi-site was used (http://www.mlit.go.jp/kowan/kyosin/eq.htm). The location of Ooi is shown in Figure 1. The time history of the input motion is shown in Figure 7. The maximum acceleration is less than 70 cm/s^2 and the duration is more than 6 minutes.

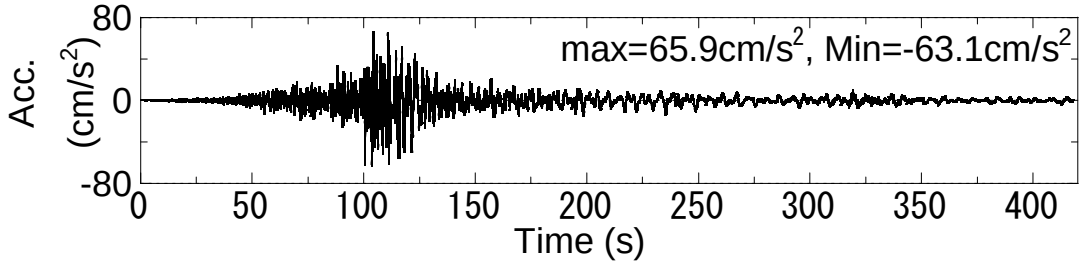

Fig.7 Input motion (seismic record: PARI)

Simulated liquefaction behavior of the two locations

Time histories of the ground responses

Figure 8 shows time histories of the accelerations, the ground surface displacement and the excess pore water pressure ratio.

The excess pore water pressure ratio at the depth of 8.5 m at site A builds up gradually and reaches almost 1.0 or liquefies after more than 100 seconds. On the other hand, the excess pore water pressure ratio at site B reaches only 0.5 or does not liquefy.

Regarding the acceleration responses, the input acceleration less than 70 cm/s^2 amplifies up to almost 150 cm/s^2 at the ground surface. This is consistent with the seismic record obtained around the sites. At site A, after the liquefaction triggering at around 125 seconds, the amplitude of the acceleration drastically decreases due to liquefaction.

The horizontal displacement at the ground surface after 125 seconds exhibits a longer period motion for long duration. The elongated period seems around 5 seconds and the double amplitude is almost 10 cm. Such an elongated period due to liquefaction cannot be seen at site B.

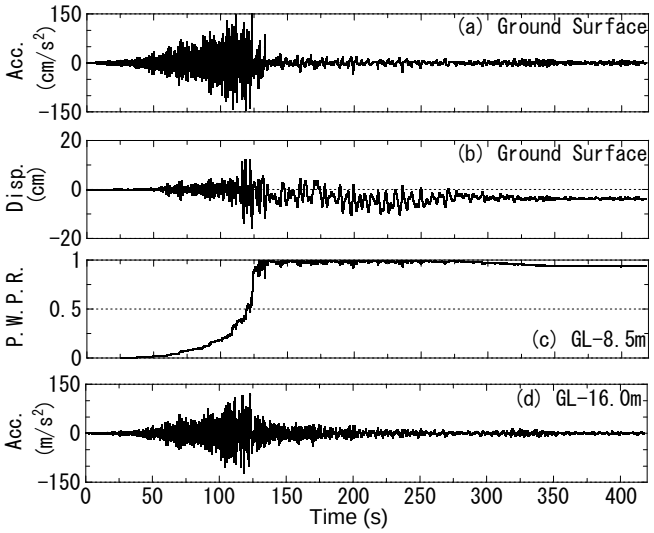

(a) Site A

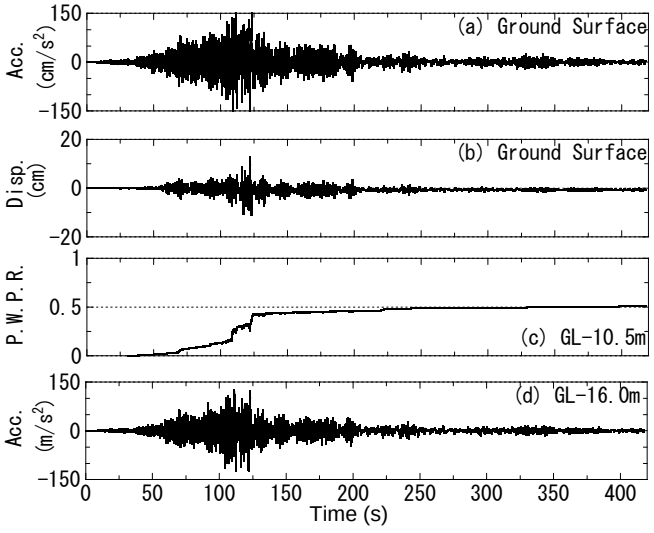

(a) Site B

Fig. 8 Time histories of responses of soil

Stress strain relation and effective stress path

Figure 9 shows the shear stress - shear strain relations and the effective stress paths of the effective stress models for both sites. The effective stress path is the relation between the mean effective stress and shear stress.

Regarding site A, the mean effective stress in the effective stress path reaches almost zero and the shear stiffness in the stress strain relation drastically decreases due to liquefaction. After triggering liquefaction, the stress-strain relation exhibits some inverse S shaped behaviors. On the other hand, the stress-strain relation of site B does not exhibit such behaviors.

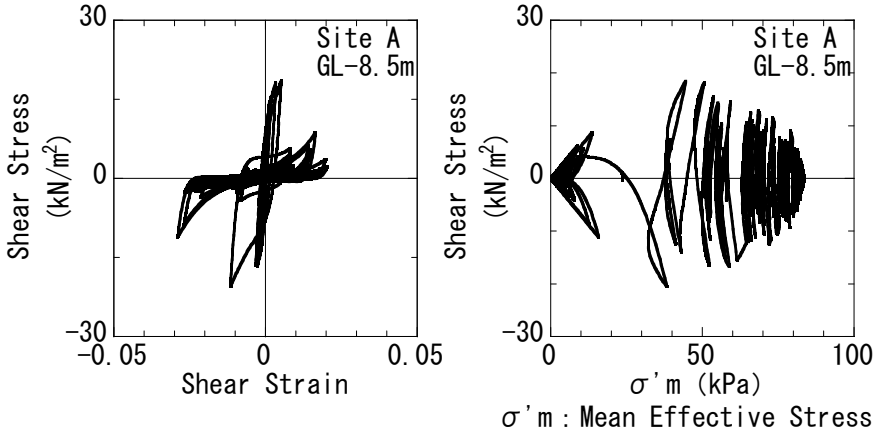

(a) Site A

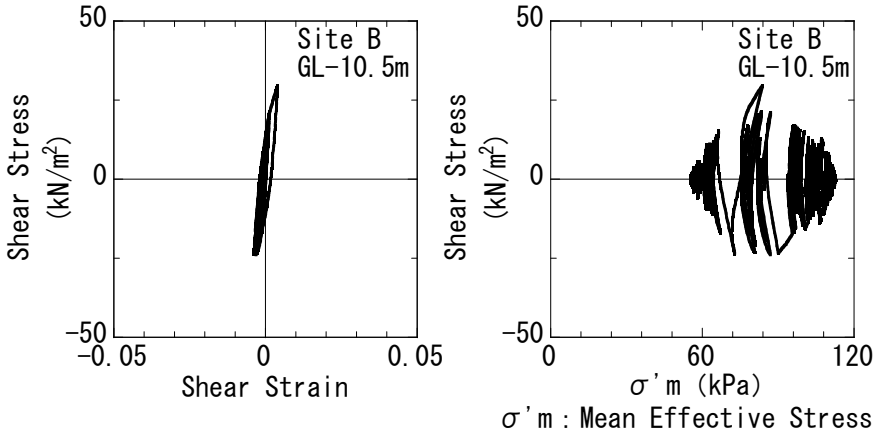

(b) Site B

Fig. 9 Stress-strain relation and effective stress pass

Vertical distributions of maximum soil responses

Figure 10 shows vertical distributions of maximum responses of soil. The soil profile and SPT-N values are also presented. The major difference between site A and site B can be seen in the maximum shear strains at the liquefied layers.

The maximum horizontal displacement at the ground surface of site A is about 16 cm and that at site B is about 13 cm. The difference seems relatively small in spite of the occurrence of liquefaction. The reason for this is that the maximum displacement occurred just before the liquefaction triggering and moreover that the deformation of the underlying soft silt layers is dominant.

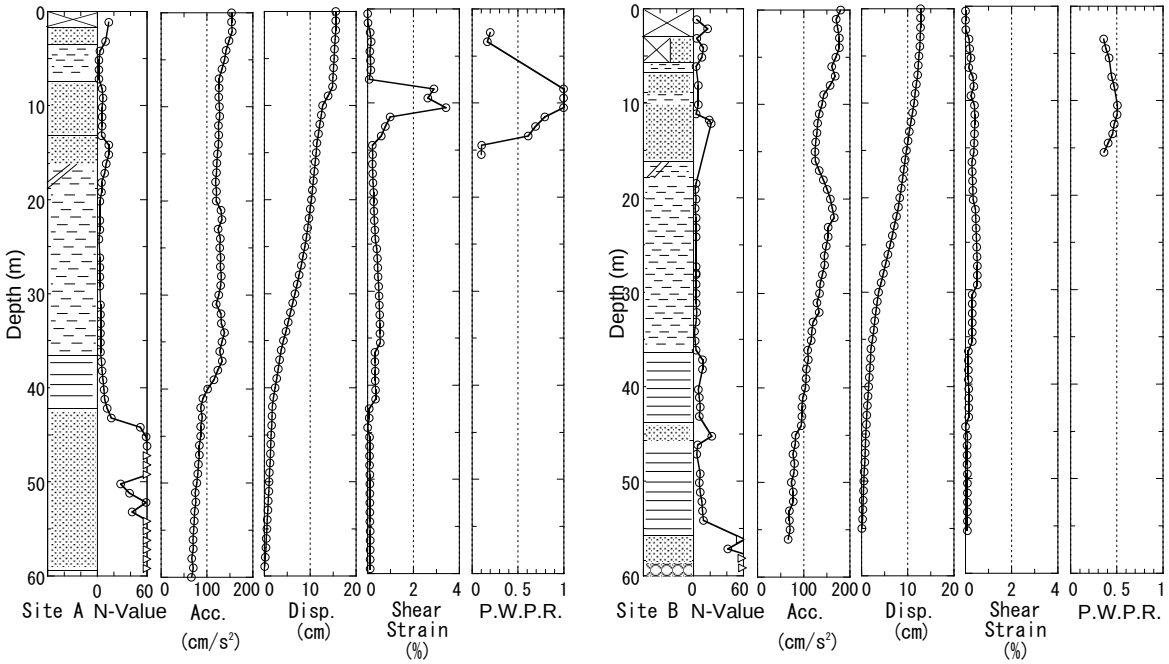

(a) Site A (b)Site B

Fig. 10 Distributions of maximum responses of soil

Factors affecting the liquefaction triggering

The most influential factor that makes the difference of the liquefaction occurrence in these simulations is the difference of the liquefaction strength of the constitutive model at large number of cycles (Figure 6). The simulation result implies that there is a possibility that the actual difference of the liquefaction strength could affect the actual liquefaction extent. However, the bases of determining the liquefaction strength for both sites are not even (i.e. The basis for site A is the combination of SPT-N value and the fines content Fc, and the basis for site B is the laboratory testing.). Therefore, we cannot conclude that the difference of the liquefaction strength is the only factor. Further experimental research on the actual liquefaction strength of the liquefiable layers is necessary.

The other possible factors that could affect the evaluation of liquefaction extent are the borderline between the reclaimed layer and the underlying natural deposit, the site effect due to the soil structure below the liquefiable layers, the evaluation of underground water level, and the aging effect on the liquefaction strength. Further research on these factors is also necessary.

Factors affecting the extent of liquefaction damage

As shown in Figure 8(a), the relatively large displacement lasted for long duration after the liquefaction triggering. This means that many times of cyclic deformation occurred in the liquefied layer. This post-liquefaction cyclic deformation could be a factor that caused the heavy liquefaction damage.

Another factor that is not considered in this research is the effect of the aftershock that occurred about 30 minutes after the main shock. The research on the liquefaction during the aftershock is also necessary.

CONCLUSIONS

The effective stress analyses of the liquefiable reclaimed ground at two locations along Tokyo Bay

coast were conducted. One location liquefied and another did not liquefy during the Great East Japan earthquake. The seismic input motion is relatively small due to the long distance from the epicenter, but has long duration due to the large magnitude. It was found that a small difference of liquefaction strength could cause a large difference of liquefaction extent. Especially the relatively low liquefaction strength at large cyclic numbers is important to evaluate the liquefaction extent for the relatively small but long seismic input motion.

ACKNOWLEDGMENTS

The input acceleration used in this research is a seismic record obtained by Port and Airport Research Institute. The maximum acceleration used in the simplified liquefaction assessment is determined considering the K-net data obtained by National Research Institute for Earth Science and Disaster Prevention. Authors really appreciate both institutes' providing the data.

REFERENCES

Architectural Institute of Japan (2001). “Recommendations for design of building foundations.” (in Japanese)

Architectural Institute of Japan (2006). “Seismic Response Analysis and Design of Buildings Considering Dynamic Soil-Structure Interaction.” (in Japanese)

Cubrinovski, M. and Ishihara, K. (1998a) “Modelling of sand behavior based on state concept.” *Soils and Foundations*, Vol.38, No.3, 115-127

Cubrinovski, M. and Ishihara, K. (1998b), “State concept and modified elastoplasticity for sand modeling”, *Soils and Foundations*, Vol.38, No.4, 213-225